Bayesian inference based on Monte Carlo technique for multiplier of performance shaping factor

Satoshi Takeda[1]
Osaka University
Osaka, Suita, Yamadaoka 2-1, Japan
e-mail: takeda@see.eng.osaka-u.ac.jp

Takanori Kitada
Osaka University
Osaka, Suita, Yamadaoka 2-1, Japan
e-mail: kitada@see.eng.osaka-u.ac.jp

ABSTRACT

The Human Error Probabilities (HEP) can be estimated using multipliers that correspond to the level of Performance Shaping Factors (PSFs) in the Human Reliability Analysis (HRA). This paper focuses on the adjustment of multipliers through Bayesian inference based on Monte Carlo techniques using the experimental results from simulators. Markov Chain Monte Carlo (MCMC) and Bayesian Monte Carlo (BMC) are used as Bayesian inference methods based on Monte Carlo techniques. MCMC is utilized to obtain the posterior distribution of the multipliers. BMC is used for the estimation of the moments of the posterior distribution such as the mean and variance. The results obtained by MCMC and that by BMC well agree with the reference results. As a case study, the data assimilation was performed using the results of the simulator experiment of Halden reactor. The results show that the multiplier changes by the result of a particular scenario and HEP of another scenario that uses the same multiplier also changes by data assimilation. Also, in the case study, the correlation between multipliers is obtained by the data assimilation and the correlation contributes to the reduction of uncertainty of HEP.

[1] Corresponding author.

1. Introduction

Failures are generally considered inevitable in the operation of complex systems such as nuclear power plants [1]. To reduce failures in complex systems, the cause of the failure needs to be carefully analyzed and tracked down. Human factors are often involved in the failures even in cases where technical factors are the primary cause of failure in complex systems [2]. Various studies have been conducted on Human Reliability Analysis (HRA) methods, especially focusing on nuclear facilities [3-10]. In recent years, there have been efforts to compare the predictions of HRA methods with experimental data obtained using full-scale simulators [11-13].

The data assimilation method based on Bayesian theory is useful to improve the consistency with experimental data. In the field of HRA, studies using Bayesian Networks have been actively conducted in recent years [14-24]. A data assimilation process based on Bayesian Networks has been proposed for the evaluation of Performance Shaping Factors (PSFs) [25]. This Bayesian Network links scenario characteristics to PSFs reported by student operators considering calculated PSFs, the bias, and context. These approaches require the construction of the Bayesian Network which incorporates key parameters affecting the target parameter such as PSFs. As the direct application of Bayesian theory to Human Error Probability (HEP), the posterior distribution of HEP has been evaluated using experimental results of the plant simulator [26-29]. In these studies, the prior distribution of HEP is assumed and the likelihood distribution is evaluated from the experimental results. If experimental results are obtained for all scenarios required for risk analysis, necessary HEPs can be rationally prepared by these direct applications of

Bayesian theory. The HEP adjustment based on Bayesian theory indicates that non-negligible uncertainty exists in HEP. It is considered that this uncertainty is from the incompleteness of the model and parameters used in HRA.

Various challenges have been pointed out regarding the HRA models. For example, it is considered that there are correlations and overlaps in the PSFs used in SPAR-H [30], thus the need for improving the model has been highlighted [31, 32]. The correlation and overlap can be avoided by increasing the number of PSFs. However, if performance influencing factors are finely classified, the uncertainty might increase due to the lack of data related to the classified PSFs. Therefore, in practical, the number of PSFs should be adjusted considering the application of HRA [33].

There is also significant uncertainty regarding of multiplier of PSFs, primarily due to parameter and model uncertainty. For instance, the multiplier of Available time used in SPAR-H has been pointed out for overestimating HEP [34]. Additionally, SPAR-H defines the failure probability as 1 if the required time is not met, but actually, it is considered that humans can actually cope with the situation by being flexible [35]. These suggest that there is a large uncertainty in the multipliers of PSFs used in SPAR-H. It is also stated that the sources used in HRA are not infallible or infinitely generalizable [36], therefore it is important to continuously consider improvements in the parameters used in HRA, such as multipliers.

As a study related to Bayesian inference of multipliers, Y. Kim et al. proposed a method to estimate the PSF effect from the results of the reliability analysis database OPERA [37]. In their study, logistic regression was employed, assuming that the probability of human error could be expressed from a product of exponential functions. In general, the probability of human error cannot be simply represented by the product of exponential functions. For example, HEP does not exceed 1 even if there are many negative PSFs, so HEP approaches 1 as the negative effect of the PSF becomes stronger. Conversely, the HEP decreases as the positive effect of the PSF becomes stronger, but it is likely to have a lower limit [30]. Therefore, rigorously, it is considered that HEP can't be expressed as a very simple function of the multiplier.

In this study, we introduce a Bayesian data assimilation method that employs the Monte Carlo technique for providing a flexible and accurate framework for multiplier assimilation. Unlike the previous approach [37], this method is not constrained by a specific formula for calculating HEP, making it universally applicable across a range of HRA methods, even those that compute HEP using complex functions. Utilizing data from simulator experiments that include successes and failures to refine the posterior distribution of multipliers, our approach enhances the reliability of HEP assessments. As the data assimilation method for input data, methods using sensitivity coefficients [38-44] or Monte Carlo methods [45-48] are widely used in the field of reactor physics. Monte Carlo methods are often used in probabilistic risk assessment, thus Bayesian inference based on Monte Carlo techniques is considered to be suitable in practice. Therefore, in the present paper, we demonstrate the applicability of data assimilation for multipliers using two major Bayesian data assimilation methods: Markov Chain Monte Carlo (MCMC) [49] and Bayesian Monte Carlo (BMC) [50]. Also, using the results of the simulator experiment of Halden reactor, we discuss the assimilated multipliers as a case study. The paper is organized as follows: Sec. 2 provides methods of Bayesian estimation based on the Monte Carlo technique, Sec. 3 shows the numerical results, and Sec. 4 concludes this study.

2. Methods of Bayesian Estimation Based on the Monte Carlo Technique

In this section, MCMC and BMC are briefly described, along with the data assimilation process for multipliers.

2.1 Data Assimilation Method Based on MCMC

MCMC is a method that utilizes the properties of a Markov chain, irreducibility, aperiodicity, and detailed balance conditions. While it is not always necessary to hold the detailed balance condition, algorithms that satisfy this condition are commonly employed. Let us consider a vector $\boldsymbol{x} = (x_1, x_2, \dots)^{\mathrm{T}}$, where T denotes the transpose operation. A Markov chain $\boldsymbol{x}^{(0)} \to \boldsymbol{x}^{(1)} \to \cdots \to \boldsymbol{x}^{(i)} \to \boldsymbol{x}^{(i+1)}$ means that the probability of transitioning from $\boldsymbol{x}^{(i)}$ to $\boldsymbol{x}^{(i+1)}$ is dependent solely on $\boldsymbol{x}^{(i)}$, regardless of $\boldsymbol{x}^{(0)}$, $\boldsymbol{x}^{(1)}$, …, $\boldsymbol{x}^{(i-1)}$. A typical example of this is a random walk. The irreducibility implies that all pairs $\left(\boldsymbol{x}^{(i)}, \boldsymbol{x}^{(j)}\right)$ can transition to each other. The aperiodicity means that the greatest common divisor of the step count to return from $\boldsymbol{x}$ to $\boldsymbol{x}$ is 1. For instance, if we calculate $\boldsymbol{x}^{(i+1)} = \boldsymbol{x}^{(i)} + \Delta\boldsymbol{x}$ where $\Delta\boldsymbol{x}$ is a uniform random number between -1 and 1, $\boldsymbol{x}^{(i+1)}$ can return to $\boldsymbol{x}^{(i)}$ in one step when $\Delta\boldsymbol{x}$=0, and it can also return to $\boldsymbol{x}^{(i)}$ in two steps. Since it is possible to return to $\boldsymbol{x}^{(i)}$ at any step, this process is aperiodic. On the other hand, when $|\Delta\boldsymbol{x}|$ is fixed to 1, this process is no longer aperiodic since $\boldsymbol{x}^{(i+1)} \neq \boldsymbol{x}^{(i)}$. The detailed balance condition requires $\mathbb{P}(\boldsymbol{x})\mathbb{T}(\boldsymbol{x} \to \boldsymbol{x}') = \mathbb{P}(\boldsymbol{x}')\mathbb{T}(\boldsymbol{x}' \to \boldsymbol{x})$, here, $\mathbb{P}$ represents the probability, and $\mathbb{T}$ denotes the transition probability. The chain $\boldsymbol{x}^{(0)} \to \boldsymbol{x}^{(1)} \to \cdots \to \boldsymbol{x}^{(i)} \to \boldsymbol{x}^{(i+1)} \to$ converges to a stationary distribution in MCMC, and this convergence property is utilized by using the detailed balance condition in many MCMC algorithms.

The present study uses a fundamental implementation based on the Random Walk MH algorithm. The random walk MH algorithm [51, 52] was implemented based on the steps outlined in the flowchart shown in Fig. 1:

i. In the first step (step $n = 1$), the initial values of the multipliers are defined as the expectation of the prior distribution.

ii. In the next step, the candidate $\tilde{\boldsymbol{x}}$ is calculated from recent values of multipliers using the Markov chain. $\tilde{\boldsymbol{x}}$ is obtained as

$$\tilde{\boldsymbol{x}} = \boldsymbol{x}^{(n-1)} + \boldsymbol{\varepsilon}, \tag{1}$$

where, $\boldsymbol{\varepsilon}$ is a vector of the random float number obtained by the normal distribution whose expectation is zero. The standard deviation of the normal distribution is a hyperparameter of the algorithm and has a major impact on the convergence of the multiplier. The dependency of the hyperparameter on the convergence is discussed in Sec. 4.1.

iii. The acceptance probability is calculated by

$$\alpha = \min\left\{\frac{f(\tilde{\boldsymbol{x}})}{f(\boldsymbol{x}^{(n-1)})}, 1\right\}, \tag{2}$$

where, f is the target distribution. Let f be the posterior distribution, using Bayesian theory, $f(\tilde{\boldsymbol{x}})/\left(\boldsymbol{x}^{(n-1)}\right)$ shown in Eq. (2) can be rewritten as

$$\frac{f(\widetilde{\boldsymbol{x}})}{f(\boldsymbol{x}^{(n-1)})} = \left(\frac{\mathbb{P}(\boldsymbol{N},\boldsymbol{k}|\widetilde{\boldsymbol{x}})\mathbb{P}(\widetilde{\boldsymbol{x}})}{\mathbb{P}(D)}\right) \Big/ \left(\frac{\mathbb{P}\left(\boldsymbol{N},\boldsymbol{k}\middle|\boldsymbol{x}^{(n-1)}\right)\mathbb{P}\left(\boldsymbol{x}^{(n-1)}\right)}{\mathbb{P}(D)}\right)$$
$$= \frac{\mathbb{P}(\boldsymbol{N},\boldsymbol{k}|\widetilde{\boldsymbol{x}})\mathbb{P}(\widetilde{\boldsymbol{x}})}{\mathbb{P}\left(\boldsymbol{N},\boldsymbol{k}\middle|\boldsymbol{x}^{(n-1)}\right)\mathbb{P}(\boldsymbol{x}^{(n-1)})}, \tag{3}$$

where, $\boldsymbol{k}(=(k_1,k_2,\dots)^{\mathrm{T}})$ is a vector of the number of failures, $\boldsymbol{N}(=(N_1,N_2,\dots)^{\mathrm{T}})$ is the number of demands, and $\mathbb{P}(D)$ is the marginal likelihood. $\boldsymbol{k}$ and $\boldsymbol{N}$ contain the experimental results of all scenarios. Eqs. (2) and (3) show that the acceptance probability is obtained by the likelihood and the probability of $\widetilde{\boldsymbol{x}}$ and $\boldsymbol{x}^{(n-1)}$. $\mathbb{P}(\widetilde{\boldsymbol{x}})$ and $\mathbb{P}\left(\boldsymbol{x}^{(n-1)}\right)$ can be calculated by the prior distribution. In the present paper, the likelihood is calculated from binomial distribution as well as other studies that aim to obtain the prior distribution of human error probability using simulator data [26-29]. For scenario i, the likelihood is described using experimental results and the multipliers $\boldsymbol{x}$:

$$\mathbb{P}(N_i,k_i|\boldsymbol{x}) = \frac{N_i!}{k_i!\,(N_i-k_i)!} p_{hep,i}(\boldsymbol{x})^{k_i}\left(1-p_{hep,i}(\boldsymbol{x})\right)^{N_i-k_i}, \tag{4}$$

where, $p_{hep,i}(\boldsymbol{x})$ is HEP obtained by multipliers $\boldsymbol{x}$ for the scenario i. The likelihood that experiment results of all scenarios are obtained can be described as

$$\mathbb{P}(\boldsymbol{N},\boldsymbol{k}|\boldsymbol{x}) = \prod_i \mathbb{P}(N_i,k_i|\boldsymbol{x}). \tag{5}$$

iv. $\boldsymbol{x}^{(n)}$ is updated by

$$\boldsymbol{x}^{(n)} = \begin{cases} \widetilde{\boldsymbol{x}} & \text{for } \tilde{u} \le \alpha \text{ and } \widetilde{x_1}, \widetilde{x_2} \dots > 0 \\ \boldsymbol{x}^{(n-1)} & \text{otherwise} \end{cases}, \tag{6}$$

where, $\tilde{u}$ is the uniform random float number in the interval (0,1). It should be noted that $\widetilde{x_1}, \widetilde{x_2} \dots > 0$ shown in Eq. (6) is not generally used in MCMC implementations. In the present study, the proposal distribution is assumed to normally distribute, which allows for negative values. As a result, the multipliers obtained during the MCMC process may include negative values. Even if multiple values are negative, the calculated failure probability may still be positive. For instance, when HEP can be calculated as the multiplication of the nominal HEP and multipliers, if two multipliers are negative, the resulting HEP will be positive. In such cases, the likelihood might be high despite the inappropriate negative values of multipliers. Therefore, we have adopted $\widetilde{x_1}, \widetilde{x_2} \ldots > 0$ in Eq. (6) for updating $\boldsymbol{x}^{(n)}$ only when all multipliers are positive.

v. Return to ii. after increasing step number n by one.

2.2 Data Assimilation Method Based on BMC

BMC is a data assimilation technique widely used in the analysis of reactor physics and nuclear data evaluation [45-48]. BMC can estimate moments of the posterior distribution such as the mean and variance. This section provides a derivation of the method to calculate moments of the posterior distribution using BMC. Firstly, let us consider computing the expectation of the function value $f(\boldsymbol{x})$ for multipliers $\boldsymbol{x}$ which follows the prior distribution $\mathbb{P}(\boldsymbol{x})$. In the Monte Carlo calculation, the expectation is approximately expressed as

$$\mathbb{E}_{\mathbb{P}(\boldsymbol{x})}\big(f(\boldsymbol{x})\big) = \int f(\boldsymbol{x})\mathbb{P}(\boldsymbol{x})\, d\boldsymbol{x} \approx \frac{1}{M}\sum_{m=1}^{M} f(\boldsymbol{x}_m), \tag{7}$$

here, M represents the sample size in the Monte Carlo calculation, and $\boldsymbol{x}_m$ denotes the multipliers in sample m, generated according to the distribution $\mathbb{P}(\boldsymbol{x})$. Next, we consider computing the expected value of $f(\boldsymbol{x})$ for $\boldsymbol{x}$ which follows the posterior distribution $\mathbb{P}(\boldsymbol{x}|\boldsymbol{N},\boldsymbol{k})$. Similar to Eq. (7), the expectation is expressed as

$$\mathbb{E}_{\mathbb{P}(\boldsymbol{x}|\boldsymbol{N},\boldsymbol{k})}\big(f(\boldsymbol{x})\big) = \int f(\boldsymbol{x})\mathbb{P}(\boldsymbol{x}|\boldsymbol{N},\boldsymbol{k})\,d\boldsymbol{x}. \tag{8}$$

Based on the Bayesian theory, the posterior distribution of $\boldsymbol{x}$ is expressed as

$$\mathbb{P}(\boldsymbol{x}|\boldsymbol{N},\boldsymbol{k}) = \frac{\mathbb{P}(\boldsymbol{x}|\boldsymbol{N},\boldsymbol{k})\mathbb{P}(\boldsymbol{x})}{\int \mathbb{P}(\boldsymbol{x}|\boldsymbol{N},\boldsymbol{k})\mathbb{P}(\boldsymbol{x})\,d\boldsymbol{x}}. \tag{9}$$

Substituting Eq. (8) into Eq. (9) and introducing the approximation formula from the Monte Carlo calculation described in Eq. (7), we can express the expected value $\mathbb{E}_{P(\boldsymbol{x}|\boldsymbol{N},\boldsymbol{k})}\big(f(\boldsymbol{x})\big)$ as follows:

$$\begin{aligned}\mathbb{E}_{\mathbb{P}(\boldsymbol{x}|\boldsymbol{N},\boldsymbol{k})}\big(f(\boldsymbol{x})\big) &= \frac{1}{\int \mathbb{P}(\boldsymbol{x}|\boldsymbol{N},\boldsymbol{k})\mathbb{P}(\boldsymbol{x})\,d\boldsymbol{x}}\int f(\boldsymbol{x})\,\mathbb{P}(\boldsymbol{N},\boldsymbol{k}|\boldsymbol{x})\mathbb{P}(\boldsymbol{x})\,d\boldsymbol{x} \\ &\approx \frac{1}{\int \mathbb{P}(\boldsymbol{N},\boldsymbol{k}|\boldsymbol{x})\mathbb{P}(\boldsymbol{x})\,d\boldsymbol{x}}\frac{1}{M}\sum_{m=1}^{M} f(\boldsymbol{x}_m)\mathbb{P}(\boldsymbol{N},\boldsymbol{k}|\boldsymbol{x}_m).\end{aligned} \tag{10}$$

$\int \mathbb{P}(\boldsymbol{N},\boldsymbol{k}|\boldsymbol{x})\mathbb{P}(\boldsymbol{x})d\boldsymbol{x}$ shown in Eq. (10) can be expressed as follows by incorporating the approximation formula described in Eq. (7):

$$\int \mathbb{P}(\boldsymbol{N},\boldsymbol{k}|\boldsymbol{x})\mathbb{P}(\boldsymbol{x})\,d\boldsymbol{x} \approx \frac{1}{M}\sum_{m=1}^{M} \mathbb{P}(\boldsymbol{N},\boldsymbol{k}|\boldsymbol{x}_m). \tag{11}$$

By substituting Eq. (11) into Eq. (10), the expected value of $f(\boldsymbol{x})$ for $\boldsymbol{x}$ following the posterior distribution $\mathbb{P}(\boldsymbol{x}|\boldsymbol{N},\boldsymbol{k})$ can be expressed as follows:

$$\mathbb{E}_{\mathbb{P}(\boldsymbol{x}|\boldsymbol{N},\boldsymbol{k})}\big(f(\boldsymbol{x})\big) \approx \frac{\sum_{m=1}^{M} f(\boldsymbol{x}_m)\mathbb{P}(\boldsymbol{N},\boldsymbol{k}|\boldsymbol{x}_m)}{\sum_{m=1}^{M} \mathbb{P}(\boldsymbol{N},\boldsymbol{k}|\boldsymbol{x}_m)}. \tag{12}$$

We can obtain the expectation of $\boldsymbol{x}$ in the posterior distribution by defining $f(\boldsymbol{x}) = \boldsymbol{x}$. the expected value of i-th multiplier in the posterior distribution is written as

$$\mathbb{E}\left(x_{i,post}\right) = \mathbb{E}_{\mathbb{P}(\boldsymbol{x}|\boldsymbol{N},\boldsymbol{k})}(x_i) = \frac{\sum_{m=1}^{M} x_{m,i}\mathbb{P}(\boldsymbol{N},\boldsymbol{k}|\boldsymbol{x}_m)}{\sum_{m=1}^{M} \mathbb{P}(\boldsymbol{N},\boldsymbol{k}|\boldsymbol{x}_m)} \tag{13}$$

where, x_i is the i-th multiplier and $x_{m,i}$ is i-th multiplier of sample $m.$ Next, let's us consider the covariance between the i-th multiplier denoted as $x_{i,post}$, and the j-th multiplier denoted as $x_{j,post}$ in the posterior distribution. If we define $f(\boldsymbol{x}) = \left(x_i - \mathbb{E}\left(x_{i,post}\right)\right)\left(x_j - \mathbb{E}\left(x_{j,post}\right)\right)$, the expected value of $f(\boldsymbol{x})$ for $\boldsymbol{x}$ which follows the posterior distribution is the covariance between $x_{i,post}$ and $x_{j,post}$. From Eq. (12), the covariance is expressed as

$$\begin{aligned} cov\left(x_{i,post}, x_{j,post}\right) &= \mathbb{E}_{\mathbb{P}(\boldsymbol{x}|\boldsymbol{N},\boldsymbol{k})}\left(\left(x_i - \mathbb{E}\left(x_{i,post}\right)\right)\left(x_j - \mathbb{E}\left(x_{j,post}\right)\right)\right) \\ &\approx \frac{\sum_{m=1}^{M}\left(x_{m,i} - \mathbb{E}\left(x_{i,post}\right)\right)\left(x_{m,j} - \mathbb{E}\left(x_{j,post}\right)\right)\mathbb{P}(\boldsymbol{N},\boldsymbol{k}|\boldsymbol{x}_m)}{\sum_{m=1}^{M}\mathbb{P}(\boldsymbol{N},\boldsymbol{k}|\boldsymbol{x}_m)}. \end{aligned} \tag{14}$$

The likelihood $\mathbb{P}(\boldsymbol{N},\boldsymbol{k}|\boldsymbol{x}_m)$ appearing in Eqs. (13) and (14) can be obtained by Eq. (5). In BMC computation, the expected value and standard deviation of the posterior distribution can be obtained from Eqs. (13) and (14), using the sample values and their likelihoods derived from standard Monte Carlo computations. As shown above, using BMC allows us to compute higher-order moments of the posterior distribution. In Sec. 4, as the feasibility study of BMC, we mainly discuss the mean and variance, which can be computed from Eqs. (13) and (14).

A significant difference between BMC and MCMC is the sampling of multipliers in Monte Carlo calculations. MCMC performs sampling of the posterior distribution by utilizing the acceptance probabilities. Therefore, MCMC cannot determine the posterior distribution solely based on random numbers following the prior distribution and their outcomes. On the other hand, BMC only requires the use of random numbers following the prior distribution and their outcomes. Therefore, BMC allows the computation of expected values and covariation in the posterior distribution without requiring any modifications to the PRA code that utilizes random numbers following the prior distribution. While BMC provides moments such as mean and variance, MCMC provides the distribution shape and percentiles of the posterior distribution.

2.3 Assumptions for introduction of Bayesian Inference Based on Monte Carlo Techniques

As mentioned in the introduction, the innovative aspect of the methodology proposed in this manuscript is its direct application of HRA methods to conduct data assimilation for multipliers. Consequently, the methodologies shown in Sections 2.1 and 2.2 are predicated on the ability of the HRA method to accurately represent HEPs and necessitate assuming the prior distributions for the multipliers. These assumptions are detailed in this section since they are crucial for the reliability of the proposed method.

2.3.1 HRA method

It is known that HEP obtained by HRA method is highly uncertain. The reasons for this large uncertainty include the lack of data to support the evaluation of HEP, the limitations of considering human cognition, and the dependence of HEP on the HRA analyst [53]. The data used in the analysis, consideration of human cognition, and analyst-dependence vary depending on HRA method [53, 54]. Therefore, ideally, data assimilation should account for all uncertainties, including uncertainties arising from data, human cognition, and analyst-dependence. In this paper, we focus on the uncertainty from the multiplier and summarize the results using a single HRA method. It is very important to consider uncertainties other than the multiplier, and this should be studied in the future. Many Bayesian data assimilation studies have used SPAR-H [9, 27, 55-57], and this paper also summarizes the results using SPAR-H. In other words, in Sec. 3, the assumption is made that HEP is obtained by SPAR-H.

SPAR-H was developed as an improved version of the first-generation HRA method [30] and has been widely used for risk assessment in nuclear power plants. This method divides human errors into diagnosis task failures and action task failures and quantifies the failure probability for each task individually. The result of the case study using the failure of the action task is shown in Sec. 3, so here the calculation for the action task is summarized. SPAR-H utilizes eight PSFs and their multipliers, as shown in Table 1. The multiplier corresponding to the PSF level is basically multiplied by the nominal HEP. If the positive number of negative PSFs is less than 3, the HEP is calculated by

$$g(\boldsymbol{x}) = NHEP \prod_{i} x_i, \tag{15}$$

here, x_i is the i-th multiplier and $NHEP$ is the nominal HEP. The nominal HEP is 0.001 for the action task in SPAR-H. To avoid HEP becoming greater than 1, HEP for the case when the number of negative PSFs is three or more is calculated by

$$g(\boldsymbol{x}) = \frac{NHEP \prod_{i} x_i}{NHEP\left(\prod_{i} x_i - 1\right) + 1}. \tag{16}$$

2.3.2 Prior distribution of multiplier

In Bayesian inference, in general, the prior distribution does not need to be precisely defined, but it is desirable to use a valid prior distribution. In relation to the validity of the multiplier, some multipliers have been discussed in comparison with experimental results. For example, when comparing the PSF effect estimated from the experiment with the multiplier of SPAR-H, the ratio of the multipliers of Stressor between high level and extreme level is comparable to the experimental result [34]. On the other hand, a large difference was confirmed for the multiplier of Available time [34]. These results suggest that the uncertainty of the multipliers varies greatly depending on the type of PSF. The authors believe that there is not enough research to quantify the uncertainty of the prior distribution of all levels of multipliers for each PSF.

In this paper, a simple prior distribution is employed to represent the prior distribution of multipliers using a log-normal distribution, taking into consideration that multipliers should not take negative values. The expectation of this log-normal distribution is equal to the SPAR-H Multiplier. Except when the multiplier is 1, the standard deviation is fixed at 50% of the expectation to model the uncertainty of multipliers. A case that the multiplier is 1 indicates that the PSF has no impact, so the standard deviation of the multiplier is set to 0 in this case. Although the simple prior distribution is used in the present study for the discussion on the applicability of the Bayesian data assimilation method, it is desirable to discuss and use a more appropriate prior distribution for the estimation of more valid multipliers.

3. Numerical result

This section summarizes the numerical results of the data assimilation. As shown in Sec. 2, MCMC method requires the hyperparameters in the data assimilation. Since the hyperparameter has a significant impact on the convergence. in Sec. 3.1, the proper hyperparameter is discussed by using a single assimilated multiplier obtained from a single scenario. In Sec. 3.2, the verification is conducted to ensure that the posterior distribution obtained by Monte Carlo techniques coincides with the reference solution, under the assumption of having results from some scenarios. In Sec. 3.3, as a case study, data assimilation is performed using the results of Halden simulator experiments [58], and the results are discussed.

3.1 Dependency of hyperparameter on convergence in MCMC

The standard deviation of the proposal distribution used in MCMC is a hyperparameter. Generally, if the standard deviation of the proposal distribution is small, the update of the multiplier becomes infrequent, leading to increased autocorrelation and poor convergence. Conversely, when the standard deviation of the proposal distribution is large, the probability that the random multiplier is negative becomes high, resulting in a higher rejection rate since the negative multiplier is not accepted in the present study. For instance, in the initial iteration, if the standard deviation of the proposal distribution is equal to the initial value of the multiplier (in this paper, the expectation of the prior distribution of the multiplier), the probability that one of the multiplier candidates is negative is about 16%. Therefore, if Bayesian updating is performed for 8 multipliers, the probability that all multipliers are positive is only $(1 - 0.16)^8 \approx 0.25$, meaning the probability that at least one multiplier is negative is about 75%.

Since the standard deviation of the proposal distribution should depend on the magnitude of the multipliers, the standard deviation σ_{target} of the proposal distribution is defined as a constant $sigma\,ratio$ multiplied by the multiplier x_{HRA} used in HRA method:

$$\sigma_{target} = (sigma\,ratio)x_{HRA}. \tag{17}$$

In this paper, x_{HRA} represents the multiplier used in SPAR-H. The convergence of the expected value and standard deviation in the posterior distribution is investigated by changing $sigma\,ratio$ from 0.01 to 0.75.

To confirm the convergence, the result of MCMC is compared with the reference solution. The posterior distribution is obtained from the prior distribution and the likelihood by the Bayesian theory, and it is easily obtained by numerical analysis by discretization if there is only one parameter with uncertainty. Here, the prior distribution of the i-th multiplier x_i is

$$\mathbb{P}(x_i) \propto exp\left(-\frac{(ln(x_i) - \mu_i)^2}{2\sigma_i}\right), \tag{18}$$

here, μ and σ respectively represent the mean and standard deviation of the normal distribution obtained by taking the logarithm of the prior distribution. Under the condition that x_i is given, in N trials, the probability of obtaining experimental results with k failures can be expressed as

$$\mathbb{P}(N, k|x_i) = \frac{N!}{k!\,(N-k)!} p_{hep}(x_i)^k \left(1 - p_{hep}(x_i)\right)^{N-k}, \tag{19}$$

here, $p_{hep}(x_i)$ represents HEP evaluated by using x_i. Based on Bayesian theory, when experimental results with k failures are observed in N trials, and the posterior distribution of $x_i$can be expressed as

$$\begin{aligned}
&\mathbb{P}(x_i|N,k) \propto \mathbb{P}(x_i)\mathbb{P}(N,k|x_i) \\
&\propto exp\left(-\frac{(ln(x_i)-\mu_i)^2}{2\sigma_i}\right)\frac{N!}{k!\,(N-k)!}p_{hep}(x_i)^k\left(1-p_{hep}(x_i)\right)^{N-k} \\
&= \frac{exp\left(-\frac{(ln(x_i)-\mu_i)^2}{2\sigma_i}\right)\frac{N!}{k!\,(N-k)!}p_{hep}(x_i)^k\left(1-p_{hep}(x_i)\right)^{N-k}}{\int exp\left(-\frac{(ln(x_i)-\mu_i)^2}{2\sigma_i}\right)\frac{N!}{k!\,(N-k)!}p_{hep}(x_i)^k\left(1-p_{hep}(x_i)\right)^{N-k}dx_i}.
\end{aligned} \tag{20}$$

To obtain the posterior distribution exactly, the denominator integral of Eq. (20) must be evaluated over the range of -∞ to ∞. However, since the log-normal distribution is used and the multiplier does not become a very large value in this study, the reference solution is obtained by approximating the integral range to be from 0 to 1000 and discretization.

In this section, the posterior distribution is shown assuming that an experimental result with 1 failure out of 100 trials is obtained. The scenario for this experiment assumes that PSF level is nominal excluding Stressor and that only Stressor is at the extreme level. Under these conditions, HEP obtained by SPAR-H is 0.005 from Eq. (15). On the other hand, since the failure probability is 0.01 (= 1/100) from the experiment, HEP obtained by the experimental result is twice as high as the HEP obtained by SPAR-H. In this case, the multiplier for extreme level of Stressor will be updated based on Bayesian theory to make the multiplier larger. The number of iterations of MCMC is 2,000,000 in the analysis.

The convergence of the computed mean and standard deviation obtained through MCMC is presented in Figs. 2 and 3, respectively. In these figures, the reference solution is shown as dashed lines, and the reference solution for the mean is 5.46 and the standard deviation is 2.53. From Fig. 2, it can be confirmed that the mean does not stabilize even after 1,000,000 iterations when $sigma\ ratio$ = 0.01. This could be because that the Markov chain takes very small steps, which prevent it from moving around the parameter space effectively. Also, when $sigma\ ratio$ = 0.75, it can be confirmed that the mean deviates from the reference solution compared to other conditions even after 1,000,000 iterations. This could be because there's a higher probability of at least one multiplier in the candidate $\tilde{\boldsymbol{x}}$ being negative, which increases the probability of this candidate being rejected, as shown in Eq. (6). As shown in Figs. 2 and 3, the results are well converged when $sigma\ ratio$ = 0.1, 0.25, or 0.5. Therefore, in the following sections, the calculation of MCMC is performed with $sigma\ ratio$ = 0.25.

3.2 Data assimilation using a few simple experiments

This section confirms the agreement of the MCMC and BMC results with the reference solution when experimental results for some scenarios are obtained. In Sec. 3.1, a single scenario is assumed, and the likelihood is obtained using Eq. (4). On the other hand, this section considers some scenarios, so the likelihood is obtained using the multiplication shown in Eq. (5).

Scenarios A to C and their experimental results used in this section are presented in Table 2. For all scenarios, it is assumed that an experimental result with 1 failure out of 100 trials is obtained. Scenario A uses the same assumptions as Sec. 3.1. Scenario B assumes that PSF level is nominal for all PSFs except for Complexity, and that Complexity level is moderate. In Scenario C, only Experience level is assumed to be Low. HEP calculated by SPAR-H is 0.005 for Scenario A, 0.002 for Scenario B, and 0.003 for Scenario C. Among Scenarios A to C, except for the nominal level, there are no common PSF levels. Therefore, the reference solution for the multiplier of extreme level of Stressor is the same as in Sec. 3.1 since the multiplier depends solely on the results from Scenario A. Similarly, for Scenarios B and C, the reference solutions are obtained by applying Eq. (20) using the results from their respective scenarios. The number of iterations for MCMC is the same as in Sec. 3.1. The number of iterations of BNC is 200,000.

The convergence of the mean for Scenarios A to C is shown in Fig. 4, and the convergence of the standard deviation is shown in Fig. 5. In these figures, the iteration of MCMC is on the first horizontal axis and that of BMC is on the second horizontal axis. As shown in these figures, MCMC results show good agreement with the reference solution even when some scenarios are used by the likelihood of Eq. (5), and BMC also converges to the reference solution. In Figs. 4 and 5, it can be confirmed that BMC converges faster than MCMC. For example, in Figs. 4 and 5, the estimates at the 50,000th iteration of BMC are closer to the reference solution than the estimates at the 500,000th iteration of MCMC. Even with the present small adjustment in expected value and standard deviation, MCMC requires about 1,000,000 iterations for convergence. This indicates MCMC might need even more iterations to converge when the difference between prior and posterior distributions is larger.

Figure 6 shows the prior distributions and posterior distributions of the multipliers used in Scenarios A to C. BMC cannot obtain the posterior distribution directly, so the results of BMC are not shown in the figure. Figure 6 shows that the posterior distribution obtained by MCMC is in good agreement with the reference solution. Table 3 illustrates a comparison of the mean, 95th percentile, 5th percentile, and standard deviation. The 95th percentile and 5th percentile of BMC are not shown in Table 3 since BMC cannot directly obtain these percentiles. Table 3 shows that the maximum error from the reference solution is 1.1% for MCMC and 0.5% for BMC. The results of this section show that MCMC can accurately obtain the posterior distribution, and BMC can accurately obtain the moments of the posterior distribution in a relatively small number of iterations.

3.3 Data assimilation using results of Halden simulator experiments

As the case study, this section discusses the results of data assimilation using the results of Scenarios 1A, 1C, and 3 of Halden simulator experiments [58]. These results have been used in a study of data assimilation for HEP [27]. This previous data assimilation additionally uses Scenario 2 for data assimilation. In Scenario 2, PFS level of Available time is inadequate and HEP at this level is 1 regardless of other PSFs in SPAR-H. Since the contribution of each PSF cannot be quantified for Scenario 2, this scenario is excluded from the present study.

Let us briefly describe each scenario. Scenario 1 involves a total loss of feedwater followed by the Steam Generator (SG) tube rupture. For this scenario, it is assumed that the plant is operating at full power, and the main feedwater pumps will trip within 2 minutes. In Scenario 1A, the success criterion is to achieve the establishment of feedback and breeding within 45 minutes by the manual reactor trip. Scenario 1C defines the success as the isolation of the ruptured SG and the control of the pressure below the SG Power-Operated Relief Valves (PORV) setpoint in the present paper. In the experiment, this action is expected to be completed within 40 minutes after the SG tube rupture. Scenario 3 is a standard SG tube rupture scenario. The success criterion for Scenario 3 is the isolation of the ruptured SG and the control of the pressure below SG PORV setpoint before SG PORV opening.

The PSF levels and experimental results are shown in Table 4. Using the experimental results of Scenarios 1A, 1C, and 3, the data assimilation of the multiplier is performed for both BMC and MCMC. HEPs of Scenarios 1A and 3 are evaluated by Eq. (15), and HEP of Scenario 1C is evaluated by Eq. (16). As in the previous section, we set the sample size for BMC as 200,000 and for MCMC as 2,000,000.

Table 5 presents the mean and standard deviation of the multipliers after data assimilation. As shown in Table 5, the differences between the MCMC and BMC are below 0.5%, which shows a good agreement. For Scenario 1C, the experimental results showed 1 failure out of 4 trials and the failure probability is higher than HEP estimated by SPAR-H (0.167). Thus, the multiplier used in Scenario 1C is adjusted to a higher value. On the other hand, for both Scenario 1A and Scenario 3, there are no failures in the experiment, and HEP obtained from SPAR-H is only 0.0001. Since the likelihood of the experimental results of Scenarios 1A and 3 is high, the adjustment of the multiplier used only in Scenarios 1A and 1C is negligible. Among the multipliers used in the case study, the multiplier of Available time at of extra level is used only in Scenarios 1A and 1C, thus this multiplier is not adjusted significantly.

The HEP obtained from the multiplier after data assimilation is shown in Table 6. As the information on the posterior distribution, in practice, it is considered that the moments of the distribution such as the mean and variance will be stored. Therefore, in Table 6, HEP is calculated based on the mean and variance. By a Taylor expansion for the mean of HEP up to the 1st order [41], the expectation of HEP is approximately calculated by

$$\mathbb{E}(P_{HEP}) \approx g\big(\mathbb{E}(\boldsymbol{x})\big), \tag{21}$$

here, $\mathbb{E}(\boldsymbol{x})$ represents the mean of the multipliers shown in Table 5. By a Taylor expansion for the infinitesimal difference of HEP up to the 1st order [41], the variance of HEP can be approximately expressed as

$$\sigma_{HEP}{}^2 \approx \sum_i (SC_i \sigma_i)^2 + 2\sum_i \sum_{j,j\neq i} SC_i SC_j \sigma_{i,j}, \tag{22}$$

here, SC_i represents the sensitivity coefficient for the i-th multiplier with respect to HEP [41], σ_i is the standard deviation of i-th multiplier, and $\sigma_{i,j}$ is the covariance between i-th and j-th multipliers. As shown in Table 6, HEP of Scenario 1A increase by 13.1% and that of Scenario 1C increase by 22.6% by the data assimilation, while there is no significant change in Scenario 3. The Multiplier used in Scenario 1C increase after data assimilation. Also, Scenarios 1A and 1C share the multiplier of Complexity at moderate level and that of Procedures at available but poor level. Therefore, HEP of Scenario 1A increases due to the effect of data assimilation using the experimental result of Scenario 1C. This outcome demonstrates that data assimilation using a particular scenario can significantly adjust HEP for other scenarios that utilize the same multiplier.

The comparison of correlation coefficients after data assimilation is shown in Fig. 7. Generally, by the data assimilation, the negative correlation is obtained between parameters with the same sign of sensitivity coefficients and with significant adjustments by the data assimilation [40]. Excluding the multiplier of Available time at extra level, the mean of the multipliers shown in Table 5 increased by over 6%. Consequently, negative correlations are observed for these multipliers. The increase in the mean of these multipliers is less than 10%, and since the magnitude of the negative correlation conferred depends on the size of this adjustment [40], the magnitude of the negative correlation coefficients shown in Fig. 7 is below 0.1. There is no significant difference in the correlation coefficients after data assimilation between MCMC and BMC. The breakdown of the variance in HEP obtained by Eq. (24) is shown in Table 7. Since the adjustment of the multiplier used in Scenario 3 is negligible, the variance of HEP is not adjusted by the data assimilation in the scenario. As shown in Table 7, in Scenarios 1A and 1C, the variance of HEP decreases due to the contribution of covariance. This shows that the uncertainty of HEP is reduced by utilizing the covariance information of the multipliers obtained by data assimilation.

4 Conclusions

The study investigated the data assimilation method based on Monte Carlo techniques for multipliers used in HRA method, utilizing the results of simulator experiments and HEP obtained by HRA method. The random walk Metropolis-Hastings algorithm, which is a basic implementation of MCMC, and BMC which is widely used for data assimilation in nuclear data are used as data assimilation methods.

In MCMC, the standard deviation of the proposal distribution is a hyperparameter, and by setting its value based on parameter surveys, the multiplier successfully converges to the reference solution. Under the condition that that experimental results of some scenarios are given, MCMC and BMC provide results which agree with the reference results well. Also, data assimilation was performed using the simulator experiment of Halden reactor. For Scenario 1C, the experimentally obtained failure probability is higher than HEP calculated by SPAR-H. Consequently, the multiplier used in Scenario 1C is adjusted to be larger. Since Scenarios 1A and 1C share some multipliers, HEP of Scenario 1A also increases. This result indicates that data assimilation for a scenario significantly affects HEP of the other scenarios which use the same multiplier. Additionally, in the present study, it was found that data assimilation gives negative correlation between multipliers, and this negative correlation contributes to the reduction of the uncertainty of HEP.

Funding

This work was supported by JSPS KAKENHI Grant Number JP23K13524.

References

[1] Perrow, C., 1994, "The Limits of Safety: The Enhancement of a Theory of Accidents," Journal of Contingencies and Crisis Management, 2(4), pp. 212-220.

[2] French, S., Bedford, T., Pollard, S. J. T., and Soane, E., 2011, "Human reliability analysis: A critique and review for managers," Safety Science, 49(6), pp. 753-763.

[3] Čepin, M., 2019, "Contribution of Human Reliability in Power Probabilistic Safety Assessment Models Versus Shutdown Models," ASCE-ASME J Risk and Uncert in Engrg Sys Part B Mech Engrg, 6(1).

[4] Bui, H., Sakurahara, T., Reihani, S., Kee, E., and Mohaghegh, Z., 2019, "Spatiotemporal Integration of an Agent-Based First Responder Performance Model With a Fire Hazard Propagation Model for Probabilistic Risk Assessment of Nuclear Power Plants," ASCE-ASME J Risk and Uncert in Engrg Sys Part B Mech Engrg, 6(1).

[5] Kim, Y., 2020, "Considerations for generating meaningful HRA data: Lessons learned from HuREX data collection," Nuclear Engineering and Technology, 52(8), pp. 1697-1705.

[6] Jung, W., Park, J., Kim, Y., Choi, S. Y., and Kim, S., 2020, "HuREX – A framework of HRA data collection from simulators in nuclear power plants," Reliability Engineering & System Safety, 194, p. 106235.

[7] Kančev, D., 2020, "A plant-specific HRA sensitivity analysis considering dynamic operator actions and accident management actions," Nuclear Engineering and Technology, 52(9), pp. 1983-1989.

[8] Kirimoto, Y., Hirotsu, Y., Nonose, K., and Sasou, K., 2021, "Development of a human reliability analysis (HRA) guide for qualitative analysis with emphasis on narratives and models for tasks in extreme conditions," Nuclear Engineering and Technology, 53(2), pp. 376-385.

[9] Garg, V., Vinod, G., Prasad, M., Chattopadhyay, J., Smith, C., and Kant, V., 2023, "Human reliability analysis studies from simulator experiments using Bayesian inference," Reliability Engineering & System Safety, 229, p. 108846.

[10] Bui, H., Sakurahara, T., Reihani, S., Kee, E., and Mohaghegh, Z., 2024, "Probabilistic Validation: Computational Platform and Application to Fire Probabilistic Risk Assessment of Nuclear Power Plants," ASCE-ASME J Risk and Uncert in Engrg Sys Part B Mech Engrg, 10(2).

[11] Liao, H., Forester, J., Dang, V. N., Bye, A., Chang, Y. H. J., and Lois, E., 2019, "Assessment of HRA method predictions against operating crew performance: Part I: Study background, design and methodology," Reliability Engineering & System Safety, 191, p. 106509.

[12] Liao, H., Forester, J., Dang, V. N., Bye, A., Chang, Y. H. J., and Lois, E., 2019, "Assessment of HRA method predictions against operating crew performance: Part II: Overall simulator data, HRA method predictions, and intra-method comparisons," Reliability Engineering & System Safety, 191, p. 106510.

[13] Liao, H., Forester, J., Dang, V. N., Bye, A., Chang, Y. H. J., and Lois, E., 2019, "Assessment of

HRA method predictions against operating crew performance: Part III: Conclusions and achievements," Reliability Engineering & System Safety, 191, p. 106511.

[14] Groth, K. M., and Swiler, L. P., 2013, "Bridging the gap between HRA research and HRA practice: A Bayesian network version of SPAR-H," Reliability Engineering & System Safety, 115, pp. 33-42.

[15] Zwirglmaier, K., Straub, D., and Groth, K. M., 2017, "Capturing cognitive causal paths in human reliability analysis with Bayesian network models," Reliability Engineering & System Safety, 158, pp. 117-129.

[16] Groth, K. M., Smith, R., and Moradi, R., 2019, "A hybrid algorithm for developing third generation HRA methods using simulator data, causal models, and cognitive science," Reliability Engineering & System Safety, 191, p. 106507.

[17] Morais, C., Moura, R., Beer, M., and Patelli, E., 2019, "Analysis and Estimation of Human Errors From Major Accident Investigation Reports," ASCE-ASME J Risk and Uncert in Engrg Sys Part B Mech Engrg, 6(1).

[18] Kamil, M. Z., Khan, F., Song, G., and Ahmed, S., 2019, "Dynamic Risk Analysis Using Imprecise and Incomplete Information," ASCE-ASME J Risk and Uncert in Engrg Sys Part B Mech Engrg, 5(4).

[19] Abrishami, S., Khakzad, N., and Hosseini, S. M., 2020, "A data-based comparison of BN-HRA models in assessing human error probability: An offshore evacuation case study," Reliability Engineering & System Safety, 202, p. 107043.

[20] Abrishami, S., Khakzad, N., Hosseini, S. M., and van Gelder, P., 2020, "BN-SLIM: A Bayesian Network methodology for human reliability assessment based on Success Likelihood Index Method (SLIM)," Reliability Engineering & System Safety, 193, p. 106647.

[21] Dindar, S., Kaewunruen, S., and An, M., 2020, "Bayesian network-based human error reliability assessment of derailments," Reliability Engineering & System Safety, 197, p. 106825.

[22] Fan, S., Blanco-Davis, E., Yang, Z., Zhang, J., and Yan, X., 2020, "Incorporation of human factors into maritime accident analysis using a data-driven Bayesian network," Reliability Engineering & System Safety, 203, p. 107070.

[23] Pan, X., Zuo, D., Zhang, W., Hu, L., and Wang, H., 2020, "Research on Human Error Risk Evaluation Using Extended Bayesian Networks with Hybrid Data," Reliability Engineering & System Safety, p. 107336.

[24] Krymsky, V. G., and Akhmedzhanov, F. M., 2021, "Assessment of Human Reliability Under the Conditions of Uncertainty: SPAR-H Methodology Interpreted in Terms of Interval-Valued Probabilities," ASCE-ASME J Risk and Uncert in Engrg Sys Part B Mech Engrg, 7(2).

[25] Shirley, R. B., Smidts, C., and Zhao, Y., 2020, "Development of a quantitative Bayesian network mapping objective factors to subjective performance shaping factor evaluations: An example using student operators in a digital nuclear power plant simulator," Reliability Engineering & System Safety, 194, p. 106416.

[26] Sun, Z., Gong, E., Li, Z., Jiang, Y., and Xie, H., 2013, "Bayesian estimator of human error probability based on human performance data," Journal of Systems Engineering and Electronics, 24, pp. 242-249.

[27] Groth, K. M., Smith, C. L., and Swiler, L. P., 2014, "A Bayesian method for using simulator data to enhance human error probabilities assigned by existing HRA methods," Reliability Engineering & System Safety, 128, pp. 32-40.

[28] Kim, Y., Park, J., Jung, W., Choi, S. Y., and Kim, S., 2018, "Estimating the quantitative relation between PSFs and HEPs from full-scope simulator data," Reliability Engineering & System Safety, 173, pp. 12-22.

[29] Musharraf, M., Moyle, A., Khan, F., and Veitch, B., 2019, "Using Simulator Data to Facilitate Human Reliability Analysis," Journal of Offshore Mechanics and Arctic Engineering, 141(2).

[30] Gertman, D., Blackman, H., Marble, J., Byers, J., and Smith, C., 2005, "The SPAR-H human reliability analysis method," US Nuclear Regulatory Commission, 230, p. 35.

[31] Laumann, K., and Rasmussen, M., 2016, "Suggested improvements to the definitions of Standardized Plant Analysis of Risk-Human Reliability Analysis (SPAR-H) performance shaping factors, their levels and multipliers and the nominal tasks," Reliability Engineering & System Safety, 145, pp. 287-300.

[32] Park, J., Jung, W., and Kim, J., 2020, "Inter-relationships between performance shaping factors for human reliability analysis of nuclear power plants," Nuclear Engineering and Technology, 52(1), pp. 87-100.

[33] Boring, R. L., 2010, "How many performance shaping factors are necessary for human reliability analysis?," 10th International Probabilistic Safety Assessment & Management Conference (PSAM10)Seattle.

[34] Liu, P., and Li, Z., 2014, "Human Error Data Collection and Comparison with Predictions by SPAR-H," Risk Analysis, 34(9), pp. 1706-1719.

[35] Robert J. Hockey, G., 1997, "Compensatory control in the regulation of human performance under stress and high workload: A cognitive-energetical framework," Biological Psychology, 45(1), pp. 73-93.

[36] Boring, R. L., and Blackman, H. S., "The origins of the SPAR-H method's performance shaping factor multipliers," Proc. 2007 IEEE 8th Human Factors and Power Plants and HPRCT 13th Annual Meeting, pp. 177-184.

[37] Kim, Y., and Park, J., 2019, "Incorporating prior knowledge with simulation data to estimate PSF multipliers using Bayesian logistic regression," Reliability Engineering & System Safety, 189, pp. 210-217.

[38] Takeda, S., and Kitada, T., 2020, "Individual Adjustment of Independent Cross-Section Set Based on Bayesian Theory," Nuclear Science and Engineering, pp. 1-13.

[39] Takeda, T., Takeda, S., Koike, H., Kitada, T., and Sato, D., 2020, "An estimation of cross-section covariance data suitable for predicting neutronics parameters uncertainty," Annals of

Nuclear Energy, 145, p. 107534.

[40] Takeda, S., Sugihara, H., and Kitada, T., 2021, "Bayesian estimation for covariance between cross-section and errors of experiment and calculation," Annals of Nuclear Energy, 163.

[41] Takeda, S., and Kitada, T., 2021, "Simple method based on sensitivity coefficient for stochastic uncertainty analysis in probabilistic risk assessment," Reliability Engineering and System Safety, 209.

[42] Takeda, S., Shibano, R., and Kitada, T., 2021, "Cross-section adjustment method based on Bayesian theory for specific cross-section set," Journal of Nuclear Science and Technology, 58(9), pp. 999-1007.

[43] Takeda, S., and Kitada, T., 2022, "Bayesian Estimation of Cross-Section, Experimental Error, and Calculation Error: Comparison with Bias Factor Method," Nuclear Science and Engineering.

[44] Takeda, S., and Kitada, T., 2023, "Importance measure evaluation based on sensitivity coefficient for probabilistic risk assessment," Reliability Engineering and System Safety, 234.

[45] Koning, A. J., 2015, "Bayesian Monte Carlo Method for Nuclear Data Evaluation," Nuclear Data Sheets, 123, pp. 207-213.

[46] Siefman, D., Hursin, M., Rochman, D., Pelloni, S., and Pautz, A., 2018, "Stochastic vs. sensitivity-based integral parameter and nuclear data adjustments," The European Physical Journal Plus, 133(10), p. 429.

[47] Cabellos, O., and Fiorito, L., 2019, "Examples of Monte Carlo techniques applied for nuclear data uncertainty propagation," EPJ Web Conf., 211.

[48] Alhassan, E., Rochman, D., Vasiliev, A., Hursin, M., Koning, A. J., and Ferroukhi, H., 2022, "Iterative Bayesian Monte Carlo for nuclear data evaluation," Nuclear Science and Techniques, 33(4), p. 50.

[49] Metropolis, N., Rosenbluth, A. W., Rosenbluth, M. N., Teller, A. H., and Teller, E., 2004, "Equation of State Calculations by Fast Computing Machines," The Journal of Chemical Physics, 21(6), pp. 1087-1092.

[50] Smith, D., and Nuclear Engineering, D., 2008, "A unified Monte Carlo approach to fast neutron cross section data evaluation," United States.

[51] Hastings, W. K., 1970, "Monte Carlo sampling methods using Markov chains and their applications," Biometrika, 57(1), pp. 97-109.

[52] Ceferino, L., Lin, N., and Xi, D., 2023, "Bayesian updating of solar panel fragility curves and implications of higher panel strength for solar generation resilience," Reliability Engineering & System Safety, 229, p. 108896.

[53] Park, J., Arigi, A. M., and Kim, J., 2019, "A comparison of the quantification aspects of human reliability analysis methods in nuclear power plants," Annals of Nuclear Energy, 133, pp. 297-312.

[54] Zhao, Y., 2022, "A Bayesian approach to comparing human reliability analysis methods using human performance data," Reliability Engineering & System Safety, 219, p. 108213.

[55] Chen, S., Zhang, L., Qing, T., and Liu, X., 2021, "Use of Bayesian networks and improved

SPAR-H for quantitative analysis of human reliability during severe accidents mitigation process in nuclear power plant," Journal of Nuclear Science and Technology, 58(10), pp. 1099-1112.

[56] Liu, J., Zou, Y., Wang, W., Zio, E., Yuan, C., Wang, T., and Jiang, J., 2022, "A Bayesian belief network framework for nuclear power plant human reliability analysis accounting for dependencies among performance shaping factors," Reliability Engineering & System Safety, 228, p. 108766.

[57] Yan, S., Yao, K., Li, F., Wei, Y., and Tran, C. C., 2022, "Application of a Bayesian network to quantify human reliability in nuclear power plants based on the SPAR-H method," International Journal of Occupational Safety and Ergonomics, 28(4), pp. 2588-2598.

[58] John, F., Huafei, L., Vinh, D. N., Andreas, B., Lois, A., Mary, P., and Julie, M., 2016, "The U.S. HRA Empirical Study."

Figure Captions List

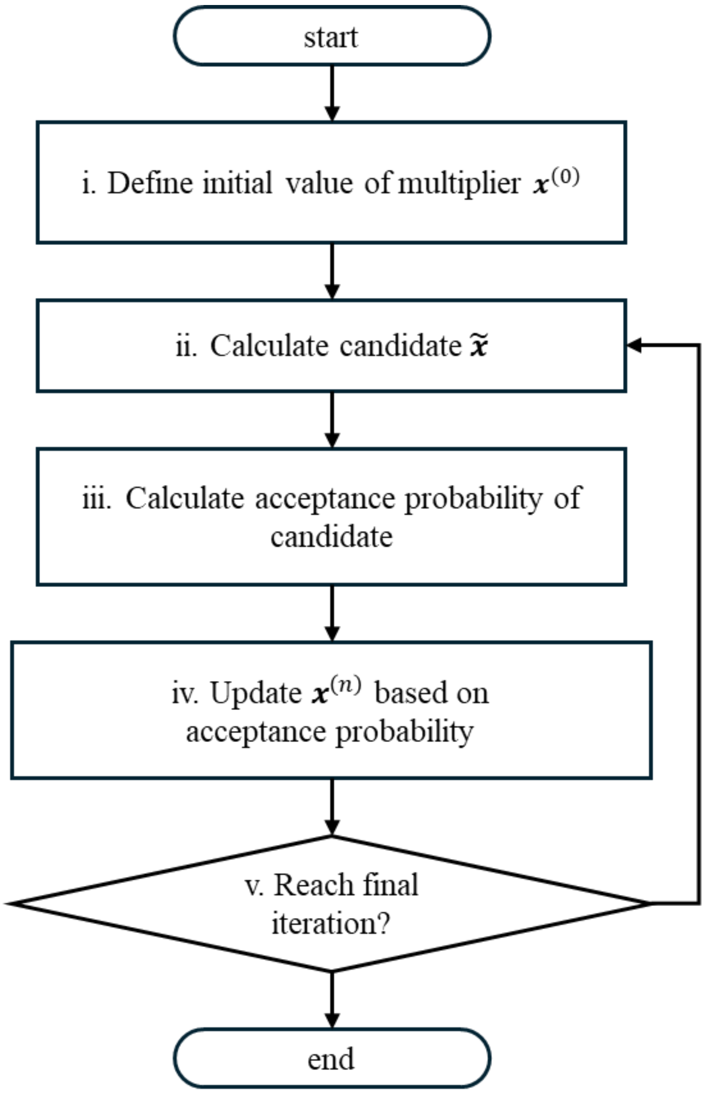

Fig.1. Flowchart of MCMC algorithm

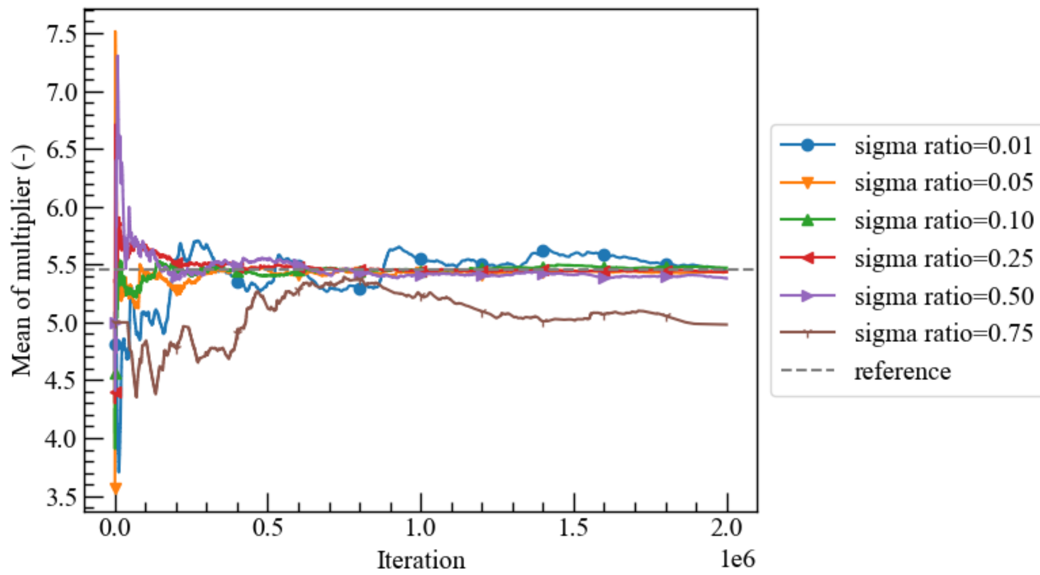

Fig.2. Convergence of mean of multiplier of Stressor at extreme level in MCMC calculation

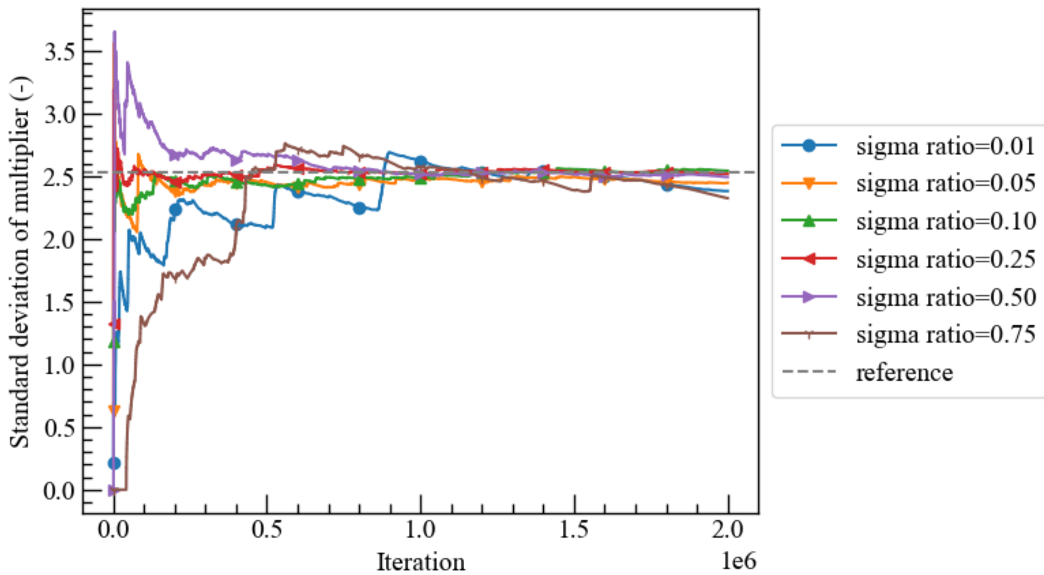

Fig.3. Convergence of standard deviation of multiplier of Stressor at extreme level in MCMC calculation

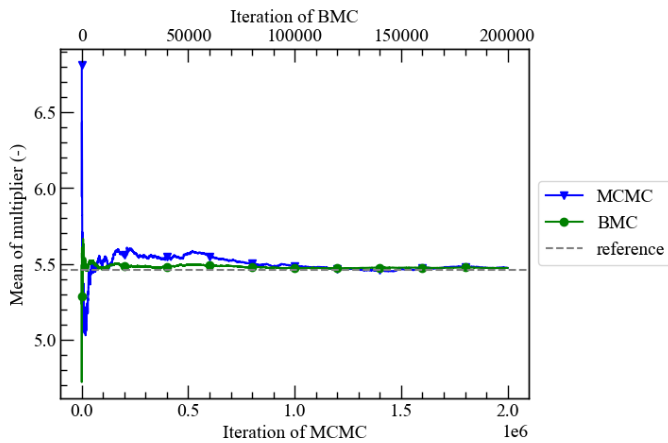

(a) Multiplier of Stressor at extreme level

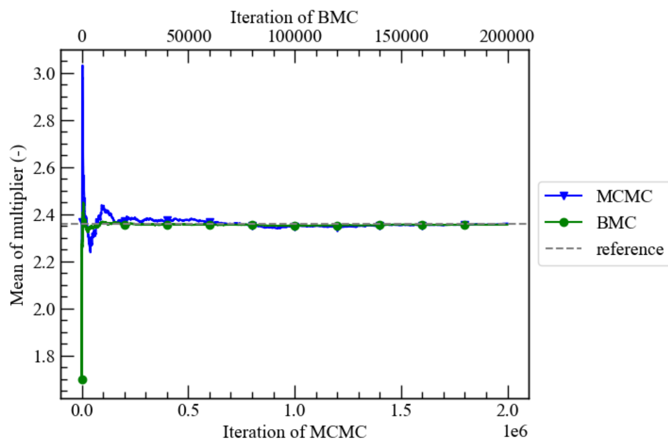

(b) Multiplier of Complexity at moderate level

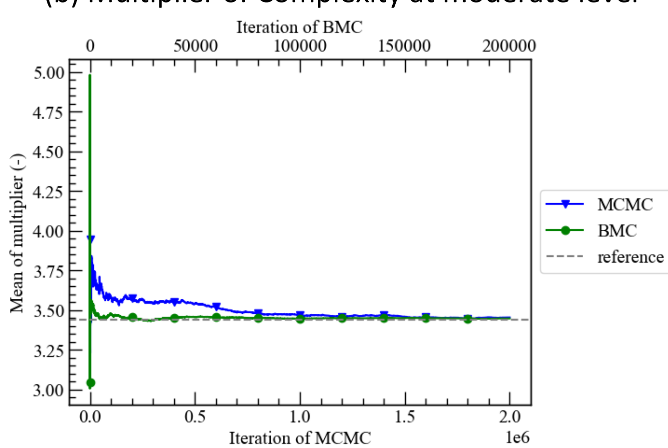

(c) Multiplier of Experience at low level

Fig.4. Convergence of mean of multiplier obtained by outcomes of scenarios A to C

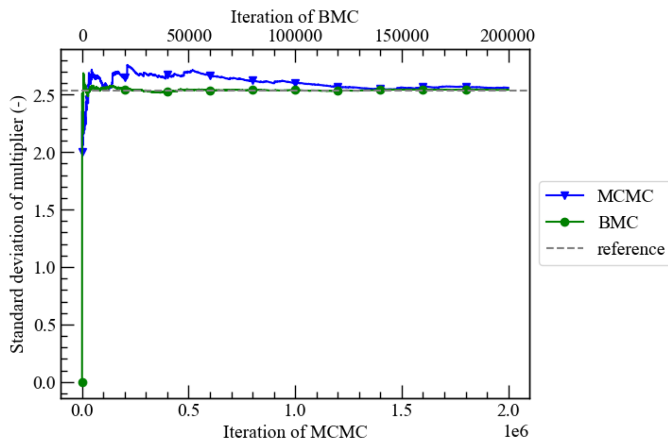

(a) Multiplier of Stressor at extreme level

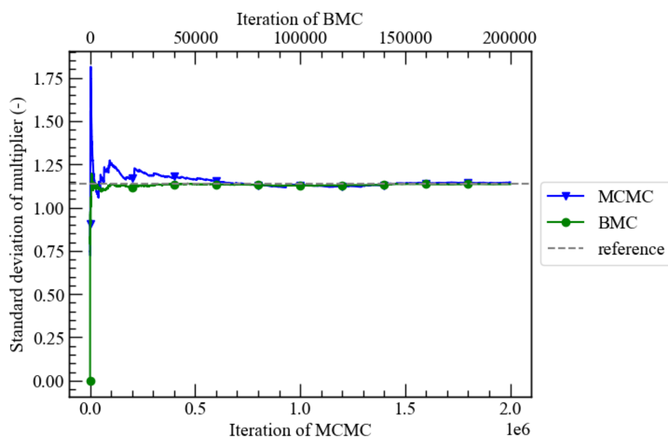

(b) Multiplier of Complexity at moderate level

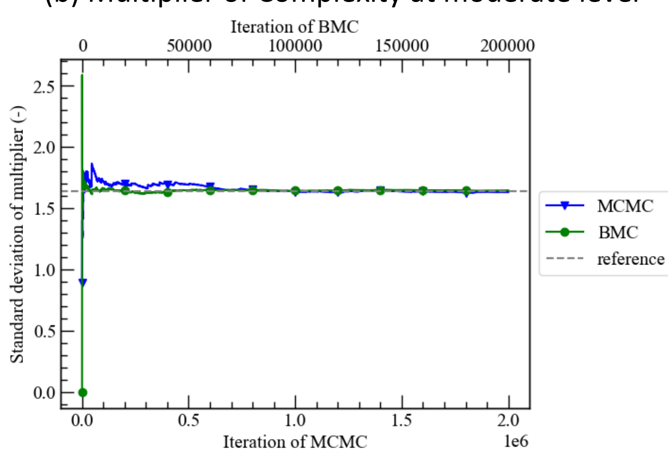

(c) Multiplier of Experience at low level

Fig.5. Convergence of standard deviation of multiplier obtained by outcomes of scenarios A to C

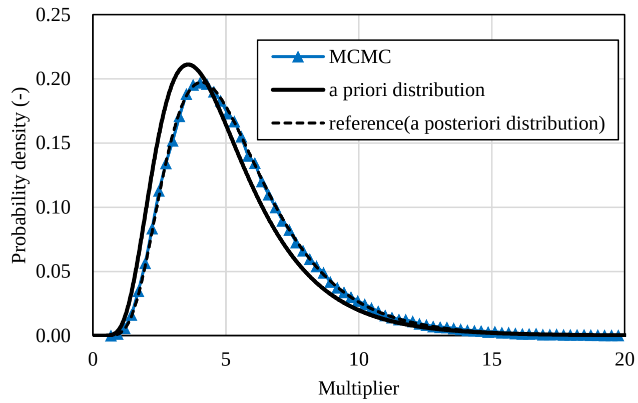

(a) Multiplier of Stressor at extreme level

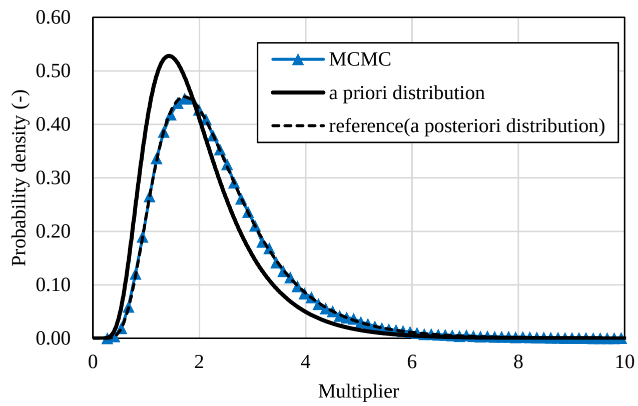

(b) Multiplier of at Complexity at moderate level

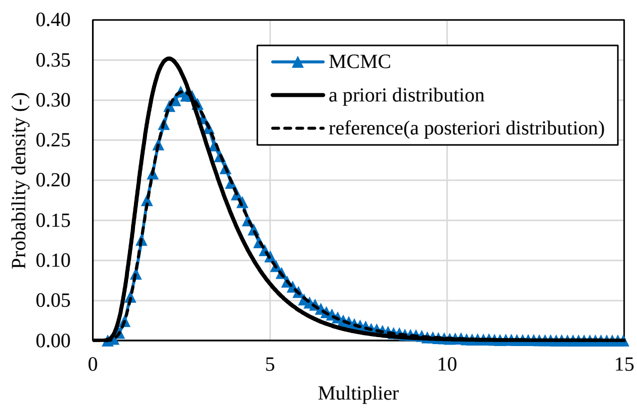

(c) Multiplier of Experience at low level

Fig.6. Comparison of probability density of multiplier

	Avail. Time Extra	Avail. Time Berely adequate	Stressor High	Complexity Moderate	Procedures Avail., but poor
Avail. Time Extra	1.00	0.00	0.00	0.00	0.00
	1.00	0.00	0.00	0.00	0.00
	0.00	0.00	0.00	0.00	0.00
Avail. Time Berely adequate	0.00	1.00	-0.08	-0.08	-0.08
	0.00	1.00	-0.08	-0.08	-0.08
	0.00	0.00	0.00	0.00	0.00
Stressor High	0.00	-0.08	1.00	-0.08	-0.09
	0.00	-0.08	1.00	-0.08	-0.08
	0.00	0.00	0.00	0.00	-0.01
Complexity Moderate	0.00	-0.08	-0.08	1.00	-0.09
	0.00	-0.08	-0.08	1.00	-0.08
	0.00	0.00	0.00	0.00	-0.01
Procedures Avail., but poor	0.00	-0.08	-0.09	-0.09	1.00
	0.00	-0.08	-0.08	-0.08	1.00
	0.00	0.00	-0.01	-0.01	0.00

MCMC
BMC
MCMC - BMC

Fig. 7. Correlation coefficient obtained by data assimilation using Halen simulator experiments

Table Caption List

Table 1 PSFs of SPAR-H and multipliers.

PSF	Level	Multiplier (Action task)
Available time	Inadequate	HEP=1.0
	Barely adequate	10
	Nominal	1
	Extra	0.1
	Expansive	0.01
Stressor	Extreme	5
	High	2
	Nominal	1
Complexity	Highly complex	5
	Moderately complex	2
	Nominal	1
Experience/Training	Low	3
	Nominal	1
	High	0.5
Procedures	Not available	50
	Incomplete	20
	Available, but poor	5
	Nominal	1
Ergonomics/HMI	Missing/Misleading	50
	Poor	10
	Nominal	1
	Good	0.5
Fitness for duty	Unfit	HEP= 1.0
	Degraded Fitness	5
	Nominal	1
Work Processes	Poor	5
	Nominal	1
	Good	0.5

Table 2 PSF of SPAR-H and outcomes of scenarios A to C.

Scen.	Avail. time	Stressors	Complex.	Exper.	Procedures	HMI	Fitness	WorkProc	Number of failures
A	Nominal	Extreme	Nominal	Nominal	Nominal	Nominal	Nominal	Nominal	1 in 100 times
B	Nominal	Nominal	Moderate	Nominal	Nominal	Nominal	Nominal	Nominal	1 in 100 times
C	Nominal	Nominal	Nominal	Low	Nominal	Nominal	Nominal	Nominal	1 in 100 times

Table 3 Comparison of multiplier obtained by outcomes of scenarios A to C.

Multiplier	Item	Reference value	MCMC		BMC	
			Value	Diff. from ref. (%)	Value	Diff. from ref. (%)
Stressor at extreme level	Mean	5.46	5.47	0.2	5.47	0.2
	95 percentile	10.25	10.34	0.8	N/A	N/A
	5 percentile	2.36	2.34	-0.7	N/A	N/A
	SD	2.53	2.56	1.1	2.54	0.5
Complexity at moderate level	Mean	2.36	2.36	0.1	2.36	-0.1
	95 percentile	4.51	4.54	0.6	N/A	N/A
	5 percentile	0.99	0.99	0.0	N/A	N/A
	SD	1.14	1.15	0.6	1.14	-0.3
Experience at low level	Mean	3.44	3.45	0.2	3.45	0.1
	95 percentile	6.54	6.61	1.0	N/A	N/A
	5 percentile	1.46	1.47	0.5	N/A	N/A
	SD	1.64	1.63	-0.5	1.64	0.4

Table 4 PSF of SPAR-H and outcomes of Halden simulator experiments.

Scen.	Avail. time	Stressor	Complex.	Exper.	Procedures	HMI	Fitness	WorkProc	Number of Failure
1A	Extra	Nominal	Moderate	Nominal	Avail. But poor	Nominal	Nominal	Nominal	0 in 4 times
1C	Barely adeq.	High	Moderate	Nominal	Avail. But poor	Nominal	Nominal	Nominal	1 in 4 times
3	Extra	Nominal	Nominal	Nominal	Nominal	Nominal	Nominal	Nominal	0 in 4 times

Table 5 Comparison of multiplier obtained by Halden simulator experiments.

PSF and level	Item	(A) Original data	MCMC		BMC		Diff. between MCMC and BMC
			(B) Value	Adjustment amount ((B)-(A))/(A) (%)	(C) Value	Adjustment amount ((C)-(A))/(A) (%)	((B)-(C))/(C) (%)
Avail. time at extra level	Mean	0.10	0.10	0.0	0.10	0.0	0.0
	SD	0.05	0.05	0.0	0.05	0.0	0.0
Avail. time at barely adeq. level	Mean	10.00	10.61	6.1	10.66	6.6	-0.5
	SD	5.00	5.07	1.4	5.07	1.4	0.0
Stressor at high level	Mean	2.00	2.13	6.5	2.13	6.5	0.0
	SD	1.00	1.01	1.0	1.01	1.0	0.0
Compexity at moderate level	Mean	2.00	2.13	6.5	2.13	6.5	0.0
	SD	1.00	1.02	2.0	1.02	2.0	0.0
Procedures at avail., but poor level	Mean	5.00	5.31	6.2	5.31	6.2	0.0
	SD	2.50	2.52	0.8	2.53	1.2	-0.4

Table 6 Comparison of HEP for scenarios of Halden simulator experiments.

Scen.	Item	(A) Original data	MCMC (B) Value	MCMC Adjustment amount ((B)-(A))/(A) (%)	BMC (C) Value	BMC Adjustment amount ((C)-(A))/(A) (%)	Diff. between MCMC and BMC ((B)-(C))/(C) (%)
1A	Mean	1.00×10^{-3}	1.13×10^{-3}	13.1	1.13×10^{-3}	13.1	0.0
	SD	8.66×10^{-4}	8.45×10^{-4}	-2.5	8.49×10^{-4}	-2.0	-0.5
1C	Mean	1.67×10^{-1}	2.04×10^{-1}	22.1	2.04×10^{-1}	22.6	-0.4
	SD	1.37×10^{-1}	1.21×10^{-1}	-12.3	1.21×10^{-1}	-12.2	-0.1
3	Mean	1.00×10^{-4}	1.00×10^{-4}	0.0	1.00×10^{-4}	0.0	0.0
	SD	5.00×10^{-5}	5.00×10^{-5}	0.0	5.00×10^{-5}	0.0	0.0

694 Table 7 Breakdown of variance of HEP.

Scenario	Method	Contribution from variance of multipliers $\left(\sum_i (SC_i\sigma_i)^2\right)$	Contribution from covariance of multipliers $\left(2\sum_i \sum_{j,j\neq i} SC_i SC_j \sigma_{i,j}\right)$	Total variance of HEP $(\sigma_{HEP}{}^2)$
1A	Original Data	7.50×10^{-7}	0	7.50×10^{-7}
	MCMC	7.59×10^{-7}	-4.58×10^{-8}	7.13×10^{-7}
	BMC	7.61×10^{-7}	-4.09×10^{-8}	7.20×10^{-7}
1C	Original Data	1.89×10^{-2}	0	1.89×10^{-2}
	MCMC	1.94×10^{-2}	-4.84×10^{-3}	1.45×10^{-2}
	BMC	1.94×10^{-2}	-4.66×10^{-3}	1.47×10^{-2}
3	Original Data	2.50×10^{-9}	0	2.50×10^{-9}
	MCMC	2.50×10^{-9}	0	2.50×10^{-9}
	BMC	2.50×10^{-9}	0	2.50×10^{-9}

695